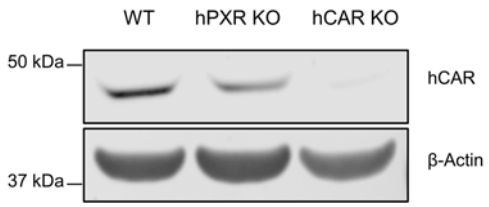

Figure S1. hPXR knockout does not increase hCAR protein level. Western blot of hCAR protein in WT, hPXR KO, and hCAR KO HepaRG cells. β-actin was used as a loading control.

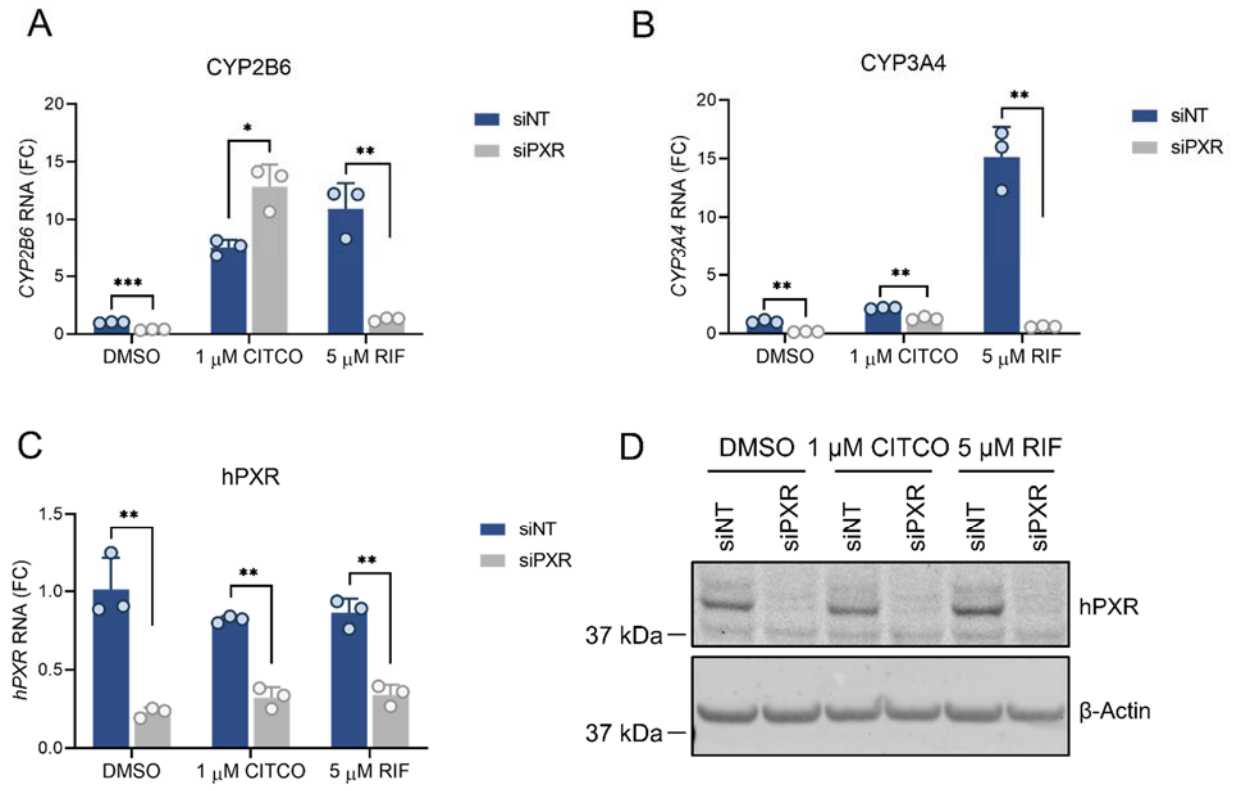

Figure S2. hPXR knockdown in primary human hepatocytes enhances agonist-induced CAR-dependent *CYP2B6* gene expression. Primary human hepatocytes (from donor #3) were treated with siNT or pooled siPXR (a pool of 4 siRNAs) at a concentration of 25 nM for 48 h then treated with the indicated compounds (0.1% DMSO, 1 μM CITCO, 5 μM RIF) for an additional 24 h. The levels of (**A**) *CYP2B6*, (**B**) *CYP3A4*, and (**C**) *hPXR* mRNA were measured by RT-qPCR. FC, fold change over siNT and DMSO treated cells. (**D**) Endogenous hPXR protein levels were determined by western blot analysis. β-Actin was used as a loading control. **P* < 0.05; ***P* < 0.005; ****P* < 0.0005.

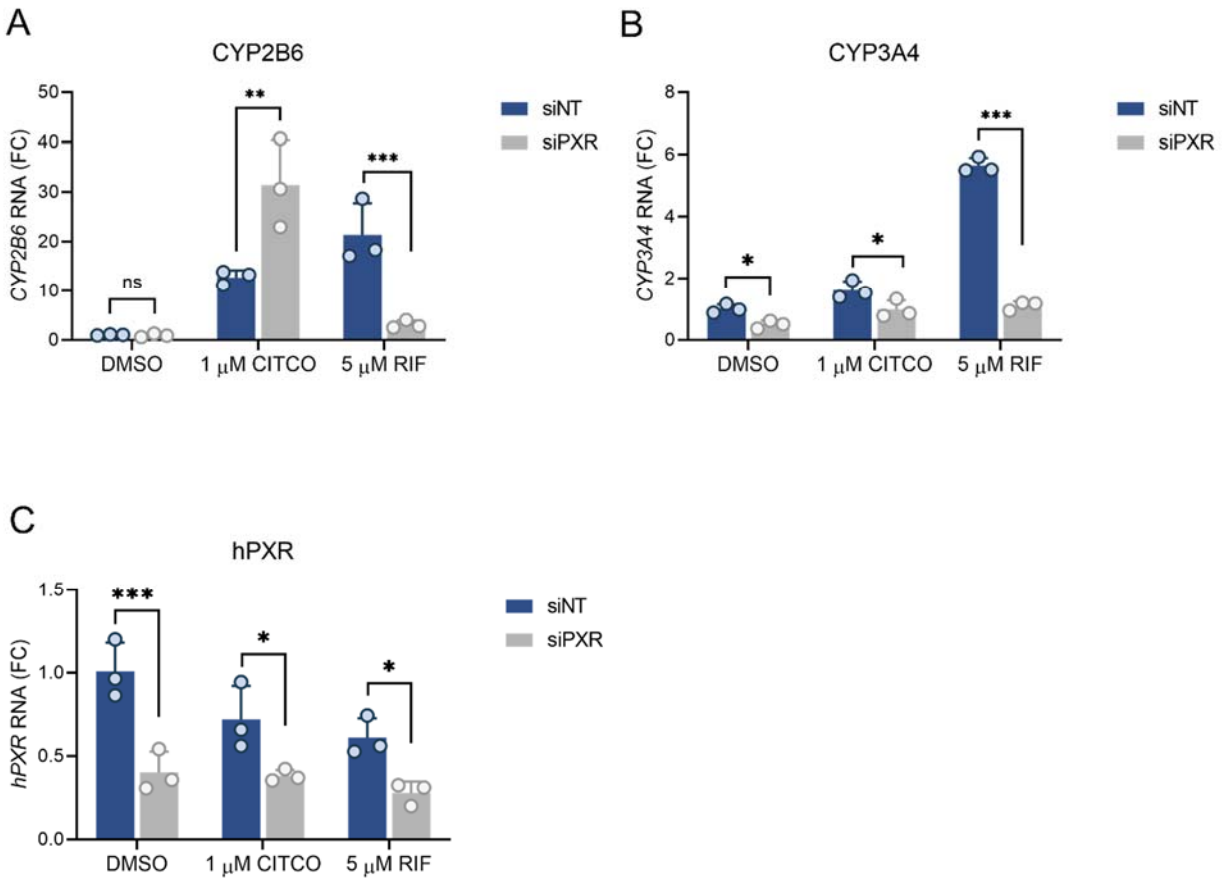

Figure S3. hPXR knockdown in primary human hepatocytes enhances agonist-induced CAR-dependent *CYP2B6* gene expression. Primary human hepatocytes (from donor #2) were treated with siNT or pooled siPXR at a concentration of 25 nM for 48 h then treated with the indicated compounds (0.1% DMSO, 1 μM CITCO, 5 μM RIF) for an additional 24 h. The levels of (**A**) *CYP2B6*, (**B**) *CYP3A4*, and (**C**) *hPXR* mRNA were measured by RT-qPCR. FC, fold change over siNT and DMSO treated cells. **P* < 0.05; ***P* < 0.005; ****P* < 0.0005; ns, not significant.

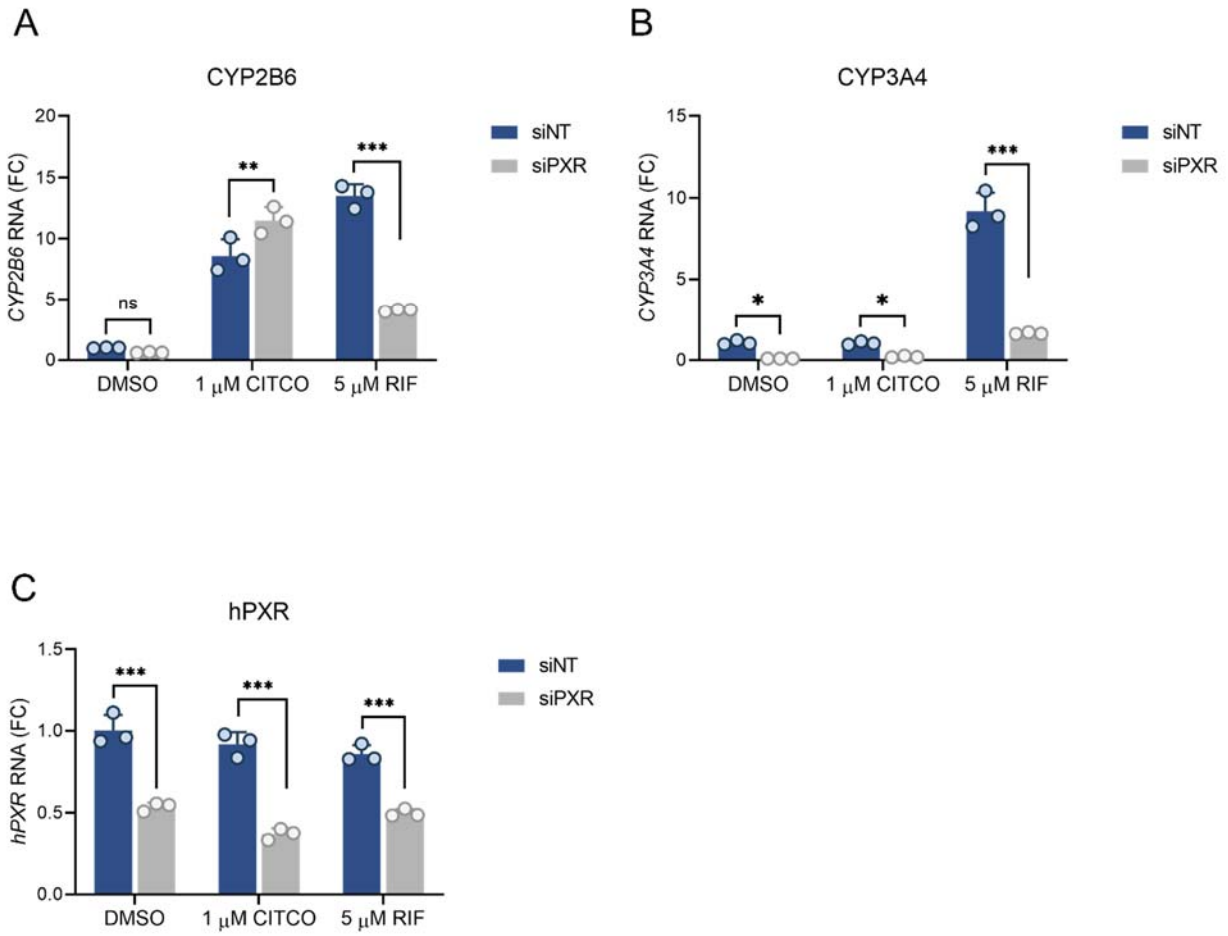

Figure S4. hPXR knockdown in primary human hepatocytes enhances agonist-induced CAR-dependent *CYP2B6* gene expression. Primary human hepatocytes (from donor #1) were treated with siNT or pooled siPXR at a concentration of 25 nM for 48 h then treated with the indicated compounds (0.1% DMSO, 1 μM CITCO, 5 μM RIF) for an additional 24 h. The levels of (**A**) *CYP2B6*, (**B**) *CYP3A4*, and (**C**) *hPXR* mRNA were measured by RT-qPCR. FC, fold change over siNT and DMSO treated cells. *$P < 0.05$; **$P < 0.005$; ***$P < 0.0005$; ns, not significant.

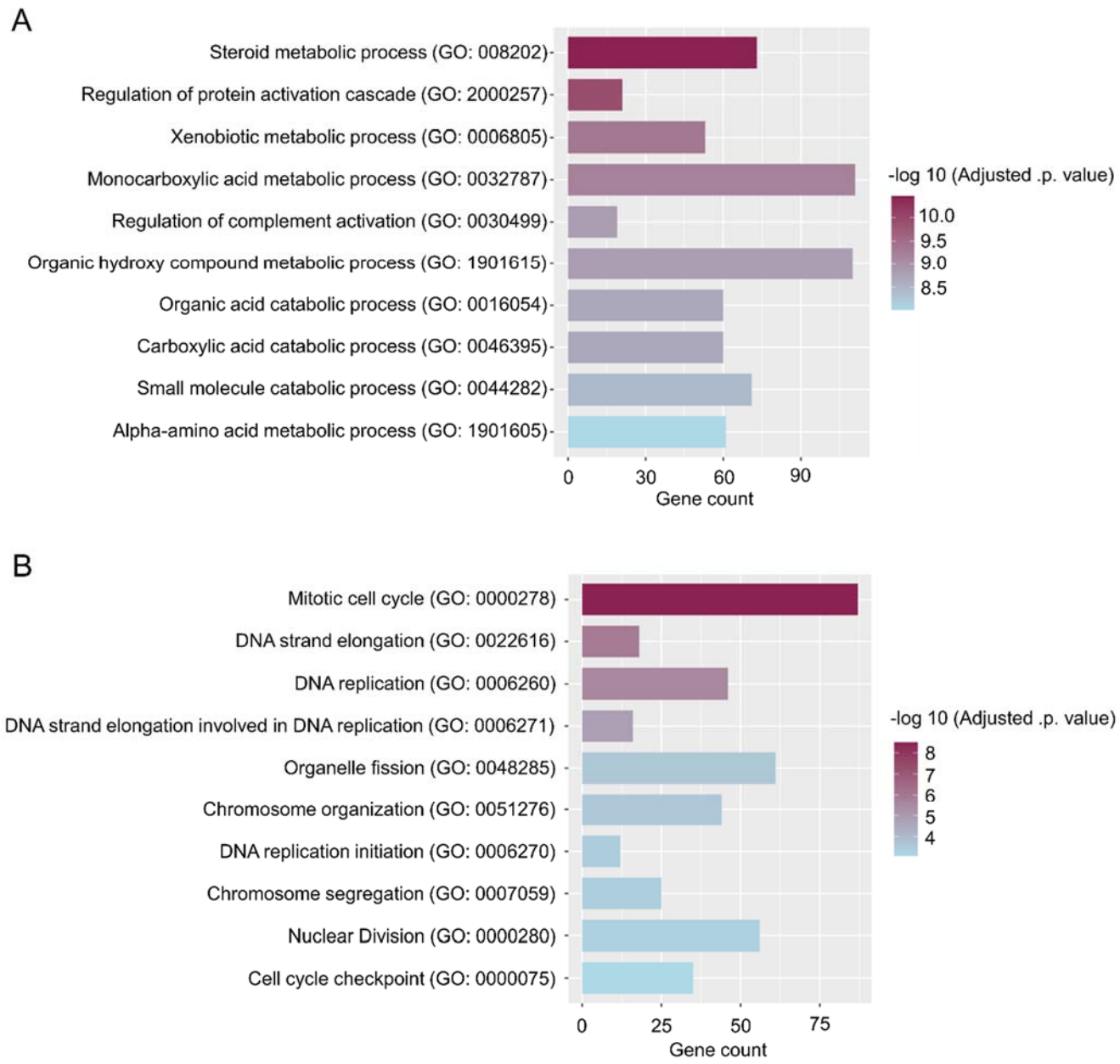

Figure S5. Depletion of hPXR alters gene expression globally. Enrichment analysis of altered pathways in hPXR KO were compared to WT control HepaRG cells. Input genes were filtered using thresholds of Log2(FC) ≥1 or ≤1 for up- or down-regulated genes, respectively. Adjusted p-values were also thresholded to values of < 0.05. Gene ontology (GO) Biological Process terms were used to query against, and results are ranked by adjusted pathway p-values. The top 10 significantly upregulated (**A**) and downregulated (**B**) pathways are listed.

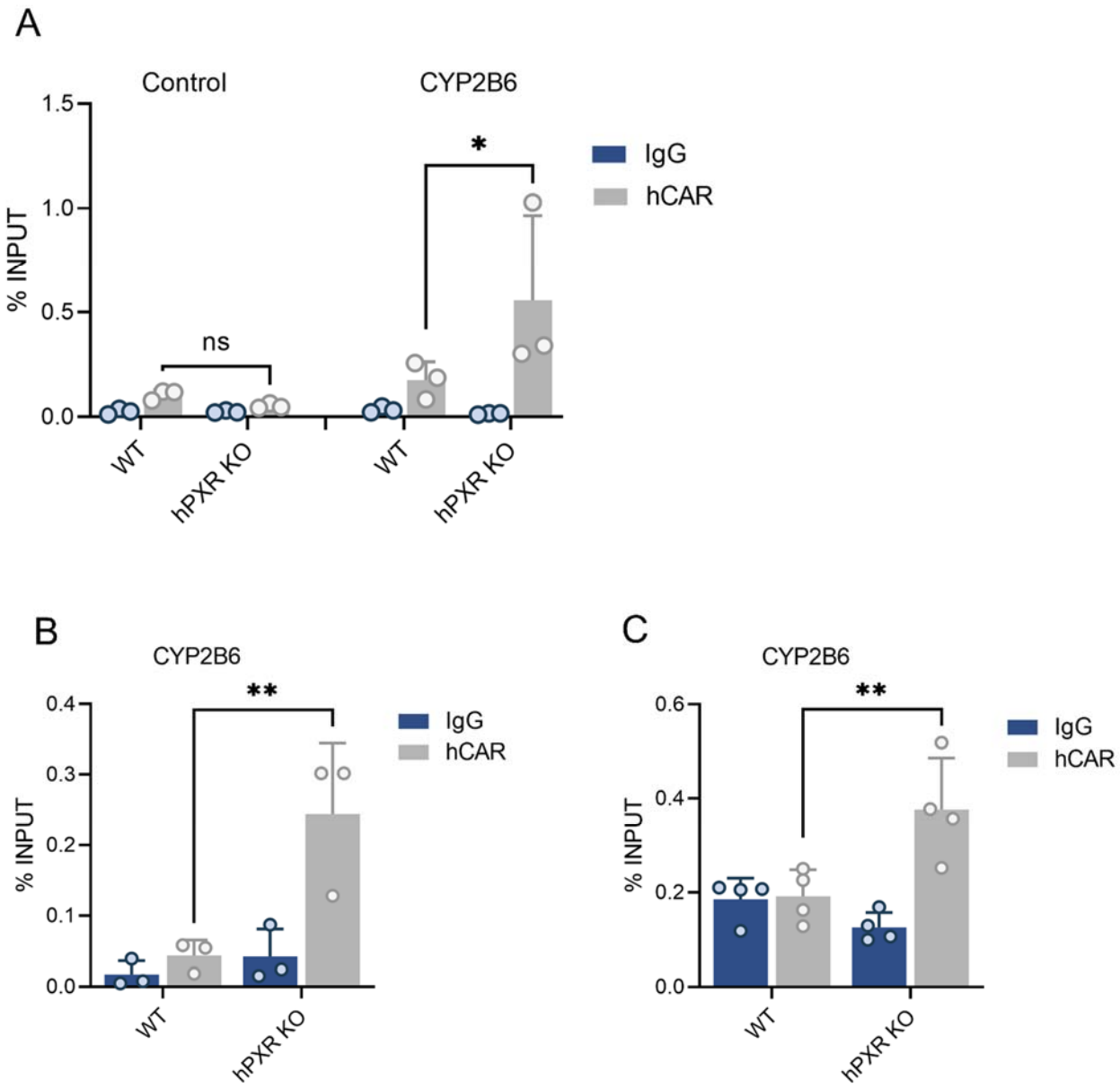

Figure S6. hPXR KO in HepaRG cells leads to increased hCAR recruitment to the endogenous *CYP2B6* promoter. (**A-C**) ChIP was performed with anti-hCAR antibody or IgG (as a negative control). Primers directed at an untranscribed genomic region (Control) (A) and the *CYP2B6* promoter (A-C) were used for qPCR. Independently differentiated cells were used in (A), (B), and (C). Data from ChIP-qPCR assay in hPXR KO cells were compared to those from the WT HepaRG cells. *$P < 0.05$; **$P < 0.005$; ns, not significant.

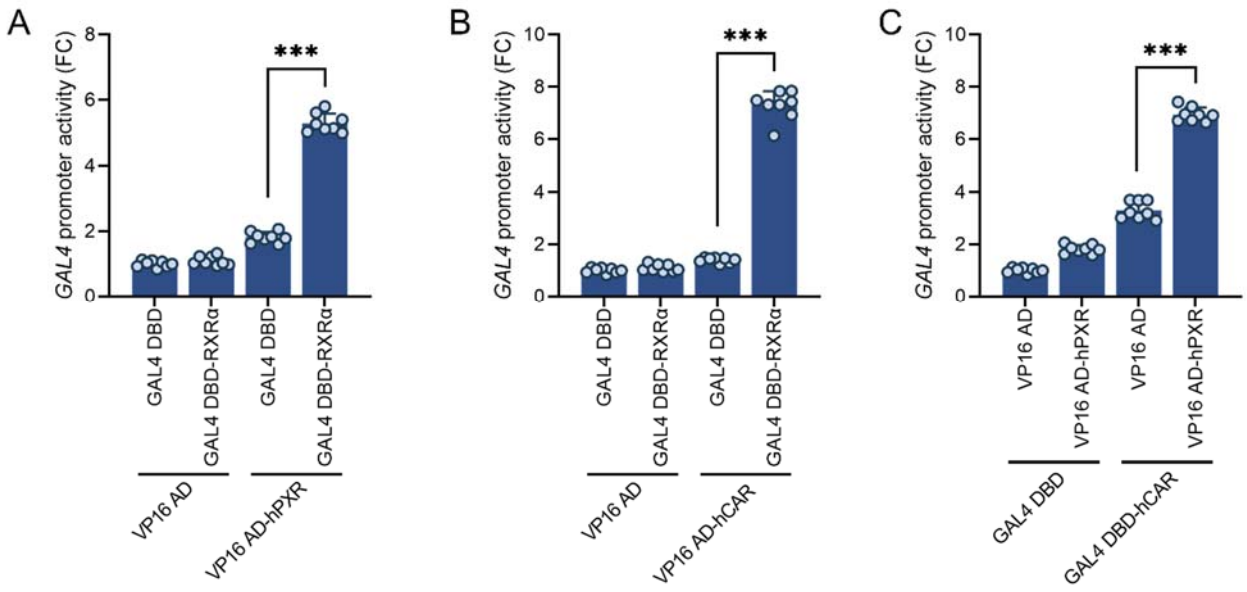

Figure S7. RXRα interacts with hPXR and hCAR. The mammalian two-hybrid assay was performed in HEK-293 cells using full-length hPXR (VP16 AD–hPXR), hCAR (GAL4 DBD–hCAR or VP16 AD–hCAR), and RXRα (GAL4 DBD–RXRα). The interaction between (**A**) hPXR and RXRα, (**B**) hCAR and RXRα, or (**C**) hPXR and hCAR was measured as the relative activity of the pG5-luc luciferase reporter, and comparisons were made as indicated at 24 h post-transfection. FC, fold change over cells transfected with GAL4 DBD and VP16 AD vectors (negative controls). *** $P < 0.0005$.

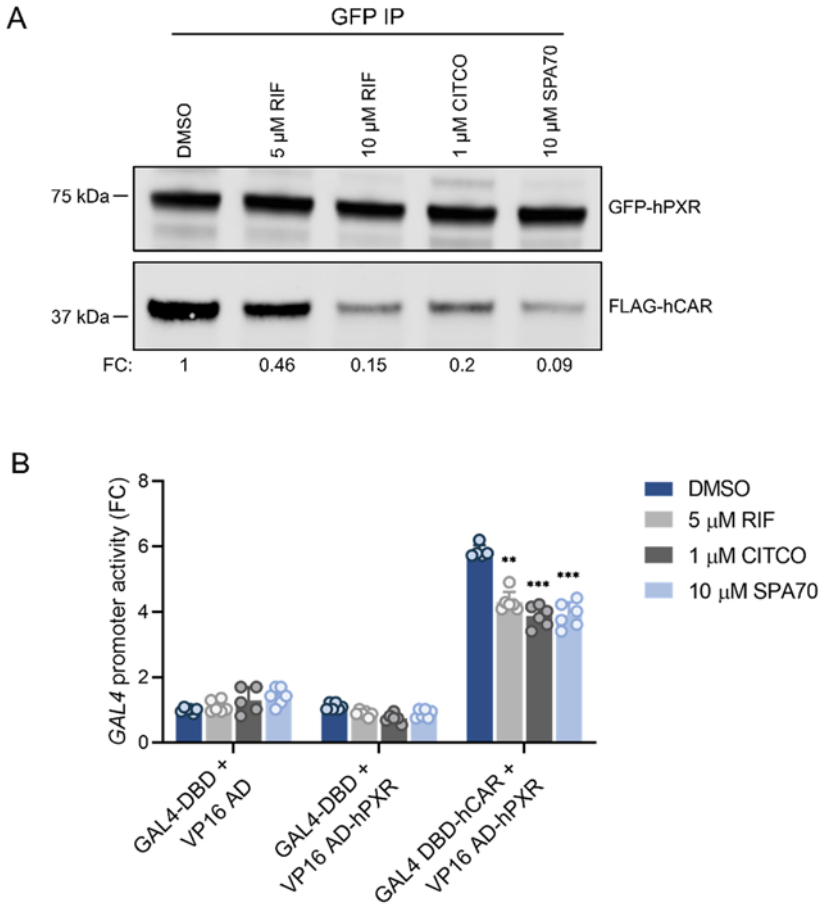

Figure S8. Receptor ligand reduces hPXR interaction with hCAR. (**A**) Receptor ligand reduces hPXR interaction with hCAR in co-IP assays. HEK-293 cells were transfected with equal amounts of GFP-hPXR and FLAG-hCAR plasmids for 24 h then treated with the indicated concentration of compound for an additional 24 h. Co-IP assays were performed using equal amounts of anti-GFP antibodies and cell lysates for each condition, and this was followed by western blot analysis with anti-GFP and anti-FLAG. Each protein band was normalized to the DMSO control. (**B**) Receptor ligand reduces hPXR interaction with hCAR in a mammalian two-hybrid assay. HEK-293 cells were transfected with the indicated plasmids. After 24 h, the cells were treated with the indicated compounds in DMSO for an additional 24 h. The relative luciferase activity was obtained by normalizing firefly luciferase to Renilla luciferase. FC, fold change over DMSO treated cells transfected with GAL4 DBD and VP16 AD vectors (negative controls). $^{**}P < 0.005$; $^{***}P < 0.0005$.

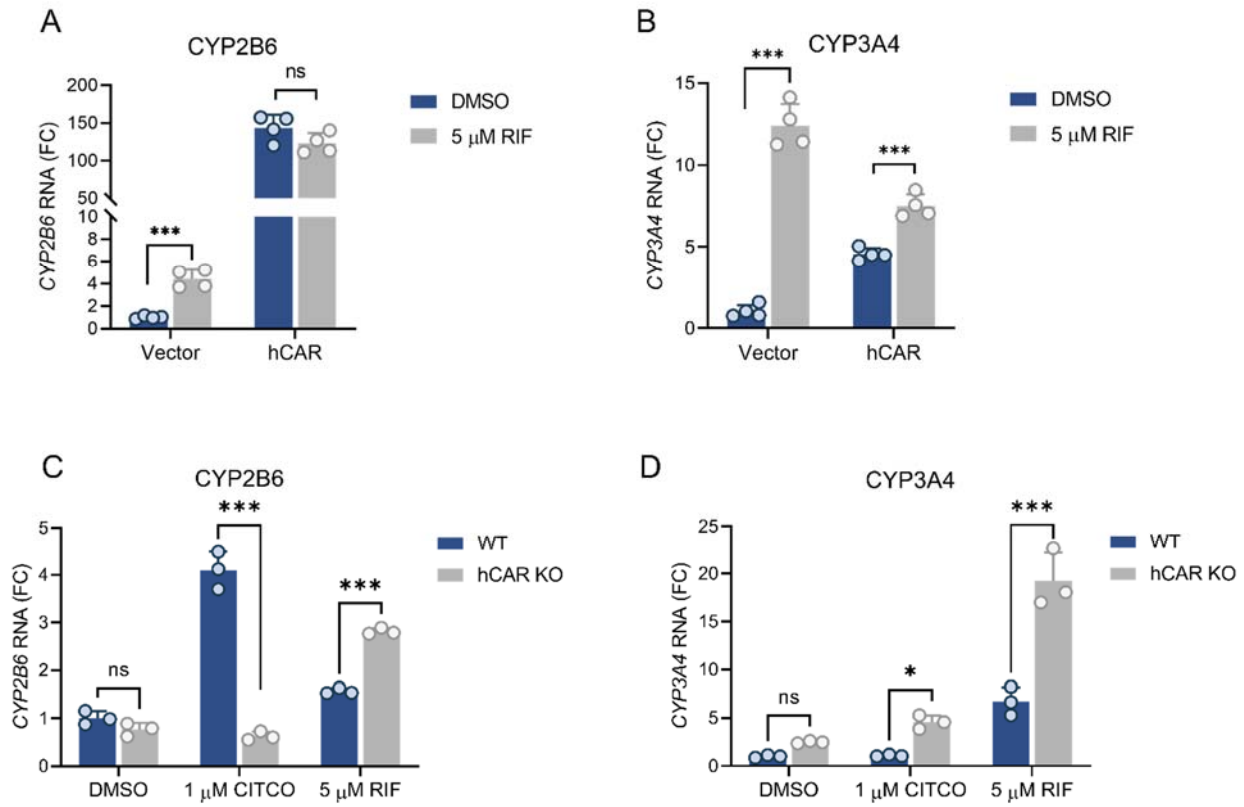

Figure S9. Overexpression of hCAR reduces, while hCAR knockout increases the inducing effect of the hPXR-specific agonist RIF on *CYP2B6* and *CYP3A4*. (**A-B**) HepaRG parental cells stably expressing empty vector control (Vector) or SF2-FLAG-hCAR (hCAR) were treated with the indicated compounds for 24 h. The *CYP2B6* (A) and *CYP3A4* (B) mRNA levels were measured by RT-qPCR. To generate the stable cells, HepaRG cells were transduced with the viruses for 24 h, after which the medium was changed, and the cells were maintained in culture for 2 weeks with a medium change every 3 days. Cells stably overexpressing hCAR or Vector were generated by puromycin (4 μg/ml) selection, starting from 1 day after viral transduction for 8 days. The cells were maintained in culture in 1% DMSO for 2 weeks to differentiate them before the assays were performed. FC, fold change over DMSO treated Vector cells. (**C-D**) *CYP2B6* (C) and *CYP3A4* (D) mRNA levels in WT cells compared to those in hCAR KO HepaRG cells treated with DMSO, 1 μM CITCO, or 5 μM Rifampicin (RIF). FC, fold change over DMSO treated WT cells. * $P < 0.05$; *** $P < 0.0005$; ns, not significant.

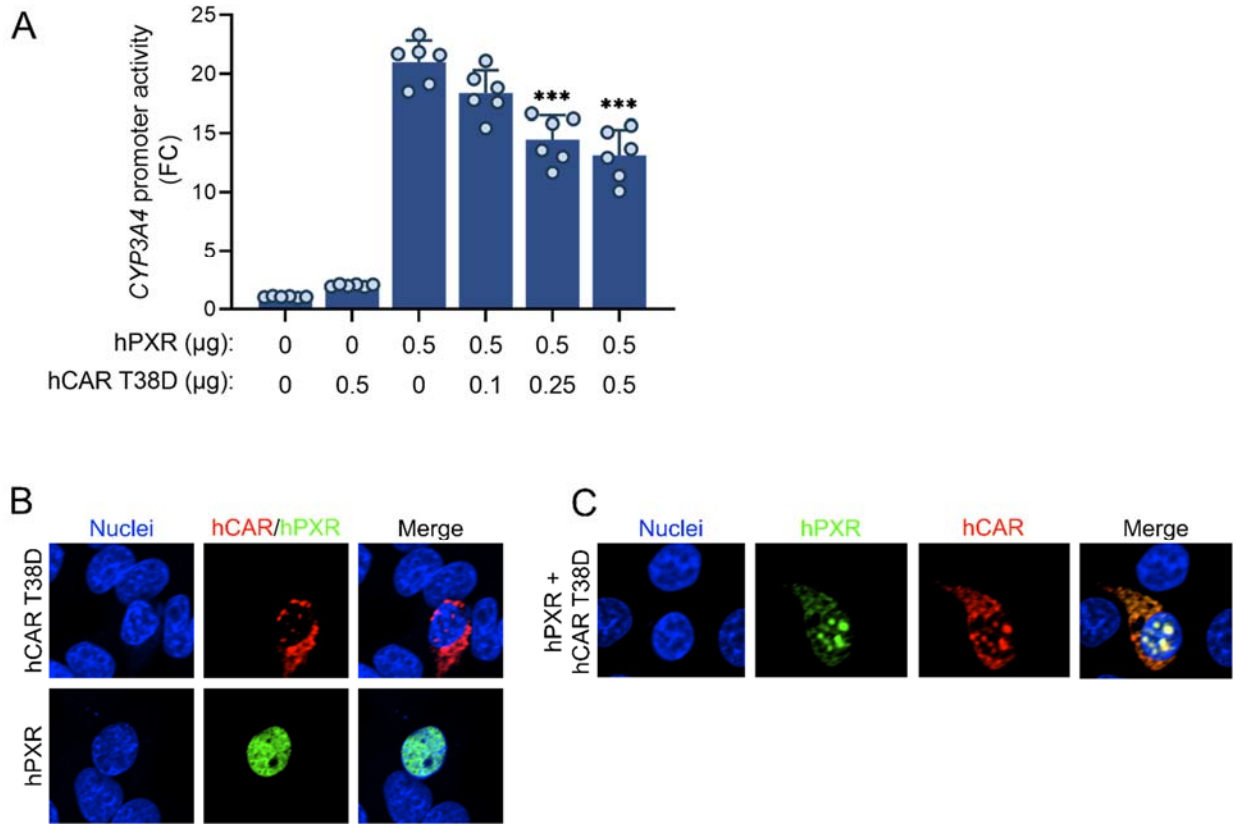

Figure S10. hCAR T38D inhibits hPXR-mediated *CYP3A4* promoter activity, and colocalizes with hPXR. (**A**) HepG2 cells were co-transfected with the *CYP3A4*-luc reporter plasmid and the TK-*Renilla* luciferase reporter (as a transfection control), along with the indicated amounts of the DNA binding–deficient FLAG-hCAR T38D mutant (hCAR T38D) and FLAG-hPXR. Firefly luciferase activity was measured at 48 h post-transfection and normalized to the *Renilla* luciferase activity. ***$P < 0.0005$. FC, fold change over cells transfected with control vector. (**B-C**) hCAR T38D co-localizes with hPXR. HepG2 cells were transfected with individual GFP-hPXR or FLAG-hCAR T38D, or co-transfected with GFP-hPXR/FLAG-hCAR T38D. This was followed by immunofluorescence staining using antibodies against FLAG (for hCAR) to determine the protein localization at 48 h post transfection. Nuclei were stained with Vybrant DyeCycle Violet Stain.

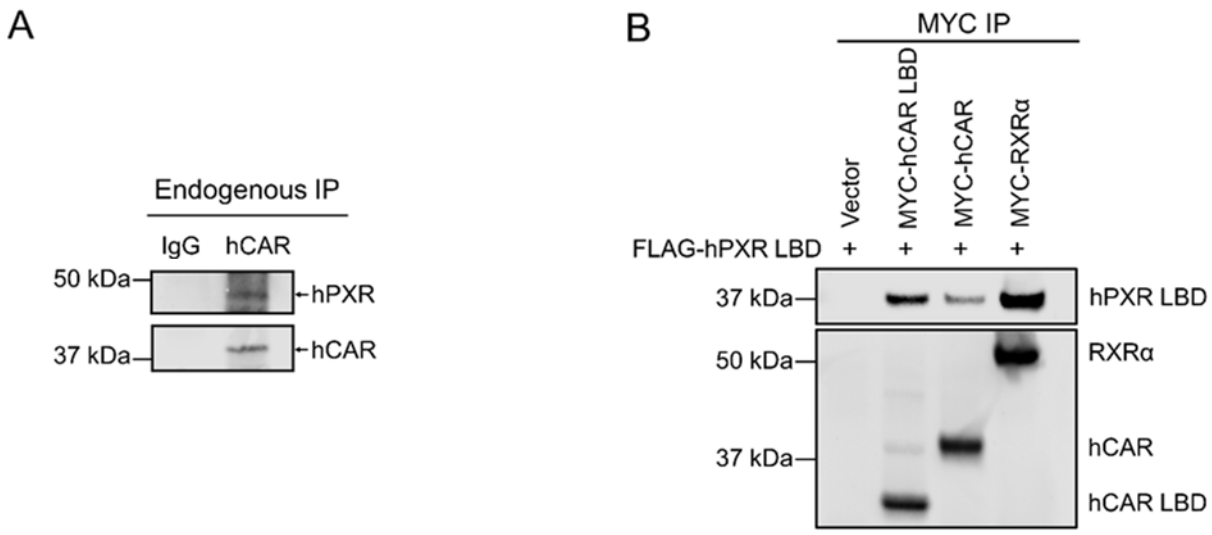

Figure S11. hCAR interacts with hPXR. (**A**) Endogenous hCAR co-immunoprecipitated with endogenous hPXR in HepaRG cells. Co-IP assay was carried out using anti-hCAR antibody. This was followed by immunoblot analysis with anti-hPXR or anti-hCAR antibodies. Immunoglobulin G (IgG) was used as a negative control. (**B**) The hPXR LBD interacts with hCAR LBD. HEK-293 cells were co-transfected with FLAG-hPXR LBD, along with vector control, MYC-hCAR LBD, MYC-hCAR, or MYC-RXRα. Co-IP assays using anti-MYC antibody were performed at 48 h post-transfection, followed by immunoblot analysis with anti-FLAG and anti-MYC.

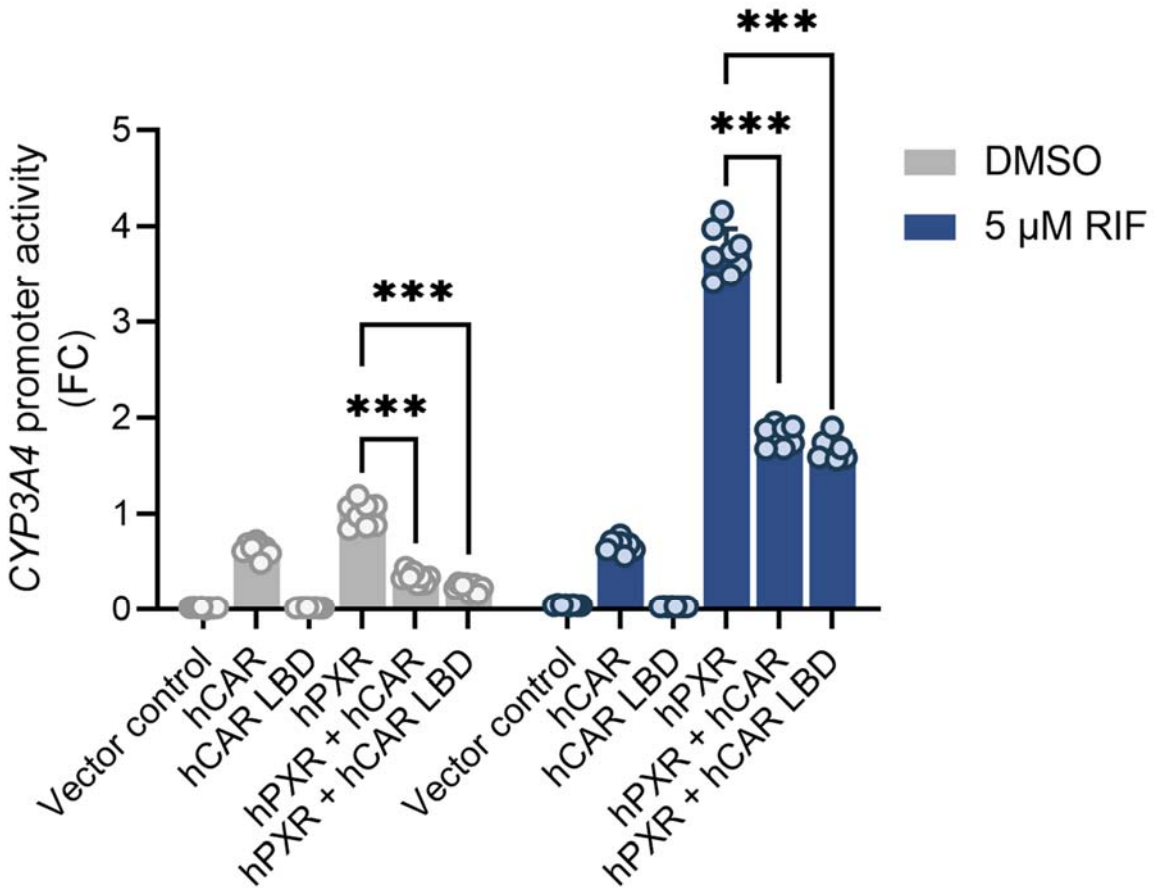

Figure S12. hCAR LBD is sufficient to inhibit hPXR transactivation of *CYP3A4* promoter. HepG2 cells were transfected with *CYP3A4* luciferase reporter in combination with vector control or hPXR (0.25 μg) with or without 0.25 μg of vector control, hCAR or hCAR LBD as shown. The cells were treated with DMSO or 5 μM RIF for 24 h, 24 h post-transfection. *CYP3A4* promoter activity was measured at 48 h post-transfection. The *CYP3A4* promoter activity resulting from hPXR and hCAR co-expression was compared to that with hPXR alone. *** $P < 0.0005$.

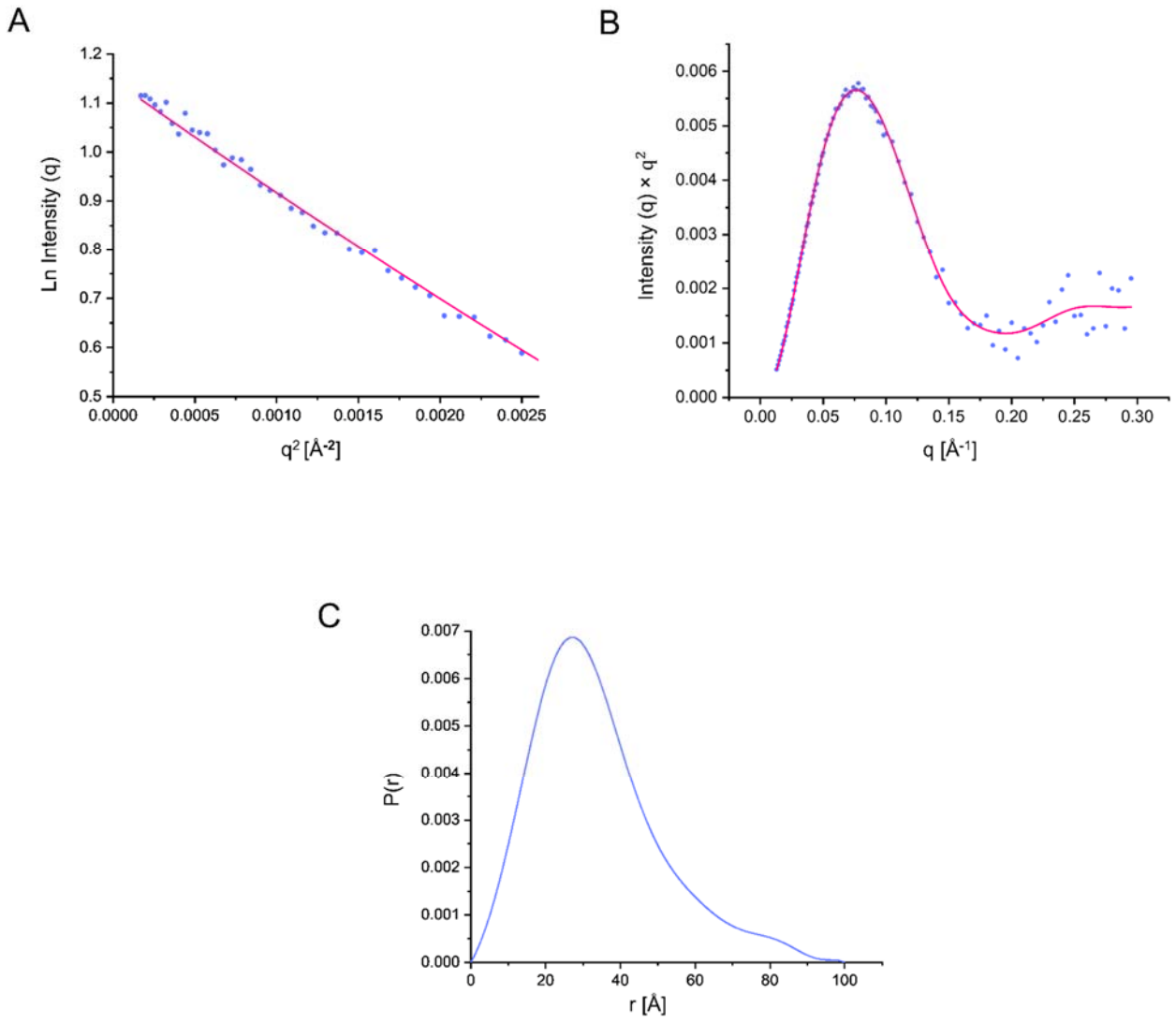

Figure S13. SAXS studies of the hPXR-hCAR heterodimer complex. (**A**) The Guinier plot was obtained from the intensity (logarithmic) as a function of q^2, where q is the momentum transfer. It is consistent with a monodisperse hPXR LBD-hCAR LBD complex with a calculated radius of gyration (Rg) of 26.67 Å. (**B**) The generated Kratky plot is characteristic of a compact and globular hPXR LBD-hCAR LBD complex. (**C**) The pair distance distribution function P(r) indicates a maximum interatomic distance (Dmax) of 100 Å within the hPXR LBD-hCAR LBD complex.

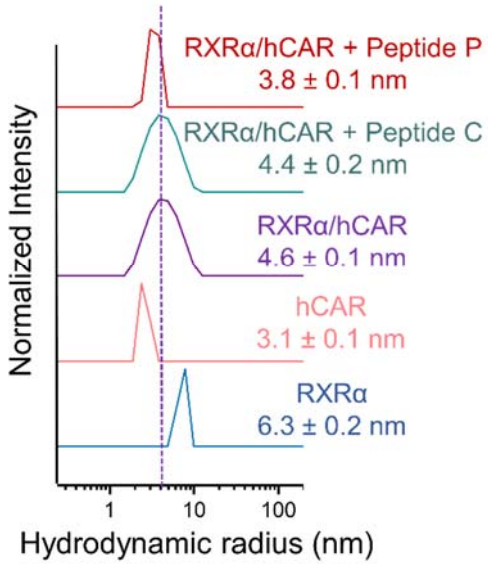

Figure S14. Dynamic light scattering (DLS) analysis illustrated as regularization histograms of hCAR LBD, RXRα LBD, and the appearance of a new species suggesting the formation of the hCAR LBD-RXRα LBD complex. The heterodimer was partially disrupted by peptide “P” (AKLLGLLAELRSINEA), but not by the mutated peptide “C” (ADLLGLLAKLDSINKA).

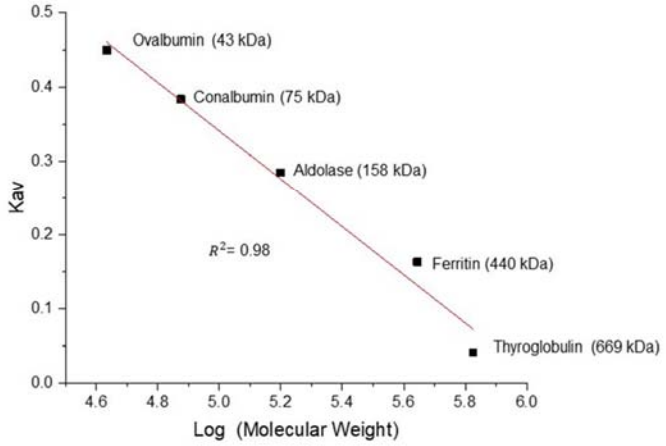

Figure S15. Size exclusion calibration curve. Calibration curve for size exclusion experiments using: ovalbumin (43 kDa), conalbumin (75 kDa), aldolase (158 kDa), ferritin (440 kDa), and thyroglobulin (669 kDa) as molecular weight standards. The plot shows the Log of molecular weight of different protein standards vs. Kav, where Kav is directly proportional to the distribution coefficient Kd and represents the fraction of the stationary phase available for diffusion of a given solute species and can be expressed as $Kav = \frac{Ve-V0}{Vt-V0}$, where Vt is the total volume of the packed column, V0 is the void volume (the elution volume of the molecules totally excluded from the pores of the beads), and Ve is the elution volume of a particular protein.

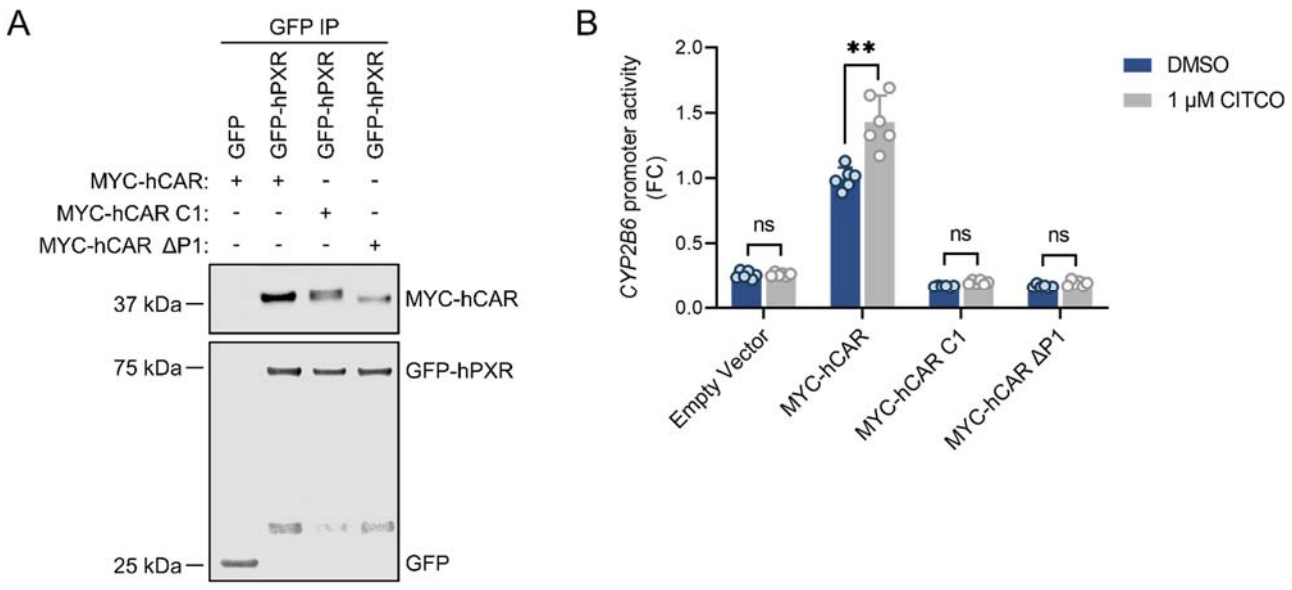

Figure S16. hCAR with the peptide P sequence (AKLLGLLAELRSINEA) mutated to (ADLLGLLAKLDSINKA) (MYC-hCAR C1) or deleted (MYC-hCAR ΔP1) decreases its activity. (**A**) MYC-hCAR C1 and MYC-hCAR ΔP1 decreases its interaction with hPXR. HEK-293 cells were co-transfected with GFP-hPXR (2 μg) and MYC-hCAR (2 μg), MYC-hCAR C1 (2 μg), or MYC-hCAR ΔP1 (2 μg), and co-IP assays were carried out at 48 h post-transfection. (**B**) MYC-hCAR C1 and MYC-hCAR ΔP1 have reduced transcriptional activity. MYC-hCAR, MYC-hCAR C1, MYC-hCAR ΔP1, or control vector (0.25 μg) was co-transfected with *CYP2B6*-luc (1 μg) into HepG2 cells. The cells were treated with DMSO or 1 μM CITCO for 24 h, 24 h post-transfection. *CYP2B6* promoter activity was measured at 48 h post-transfection. The *CYP2B6* promoter activity resulting from cells treated with CITCO was compared to that with DMSO. FC, fold change over cells transfected with vector control. ** $P < 0.005$; ns, not significant.

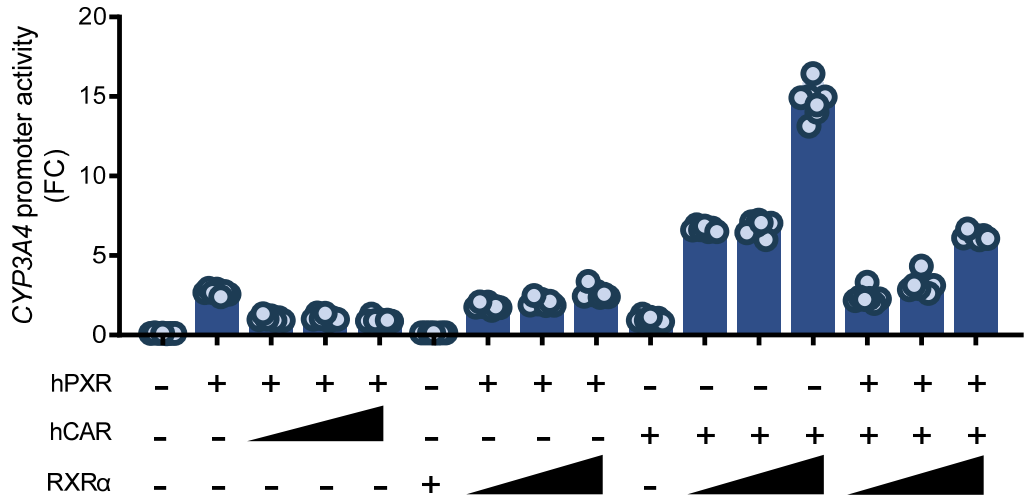

Figure S17. The transactivating activity of hCAR–RXRα on *CYP3A4* promoter is higher in the absence of hPXR than in its presence. HepG2 cells were co-transfected with *CYP3A4* luciferase reporter in combination with hPXR, hCAR, or RXRα. Triangles represent increasing receptor plasmid doses (0.05, 0.1, and 0.25 μg), (+) represents 0.25 μg of receptor plasmid, and (−) represents variable amounts of pcDNA3.1 vector control, calculated to make the total amount of transfected DNA equal. *CYP3A4* promoter activity was measured at 48 h post-transfection. FC, fold change over cells transfected with hPXR alone.

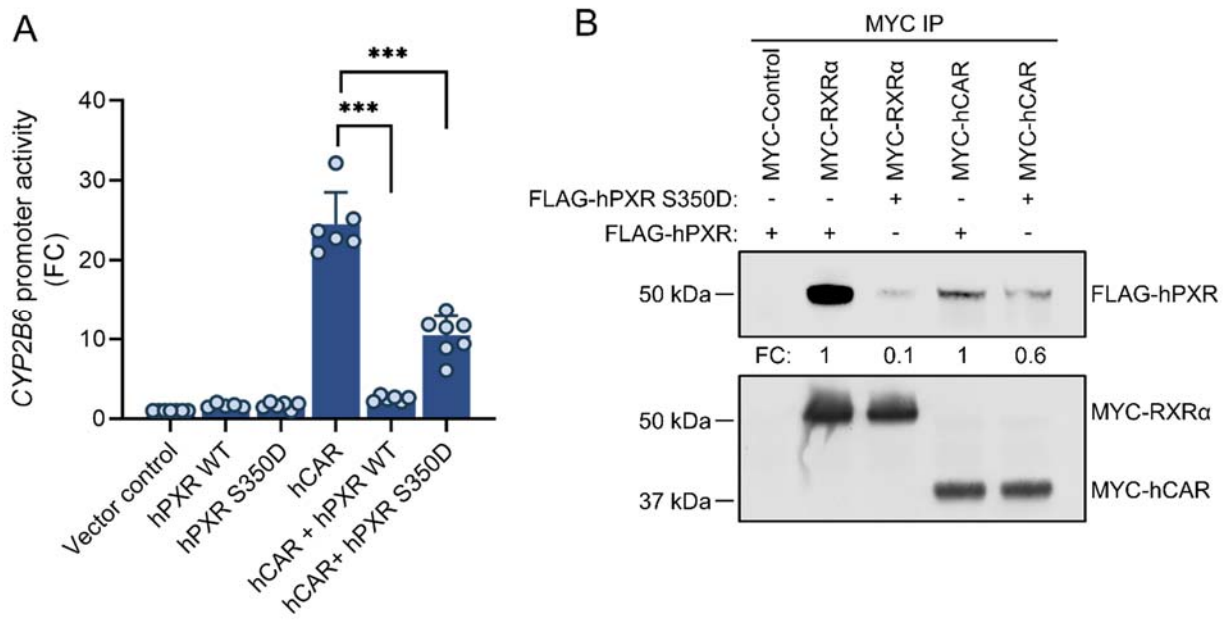

Figure S18. The hPXR S350D mutant interacts with hCAR at a reduced level. (**A**) The hPXR S350D mutant inhibits hCAR but does so at a lower level than WT hPXR. FLAG-hCAR, FLAG-hPXR WT, or FLAG-hPXR S350D, individually or combined as indicated, along with the *CYP2B6*-luc plasmid, were transfected into HepG2 cells. Luminescence was measured at 48 h post-transfection and compared to that in cells transfected with FLAG-hCAR alone. ****P* < 0.0005. FC, fold change over cells transfected with vector control. (**B**) The hPXR S350D mutant interacts with hCAR but does so at a lower level than WT hPXR. FLAG-hPXR WT or FLAG-hPXR S350D was co-expressed with either MYC-hCAR (or Vector control) or MYC-RXRα in HEK-293 cells for 48 h, after which co-IP assays were performed with anti-MYC antibodies. The proteins were subjected to western blot analysis with anti-FLAG, or anti-MYC antibodies. Each protein band was normalized to the FLAG-hPXR WT IP sample (set as 1).

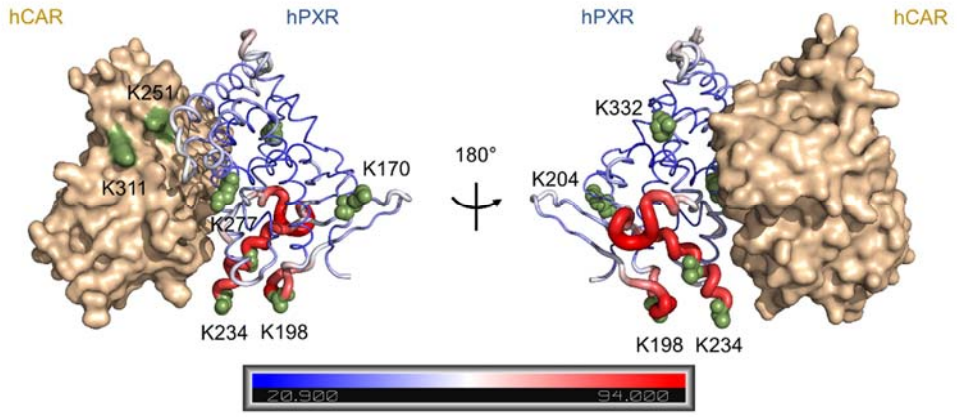

Figure S19. Crosslinking mass spectrometry data and b factor relationship. The crystal structures of hPXR LBD (PDB code 1ILH) and hCAR LBD (PDB cod 1XV9) were superimposed on the hPXR LBD-hCAR LBD model, where hCAR LBD is shown in surface representation (light brown) and hPXR LBD is represented in putty cartoon. Increasing b factor is indicated by a larger radius in the cartoon with concomitant color change. Lysine residues participating in the crosslinking are shown as green spheres.

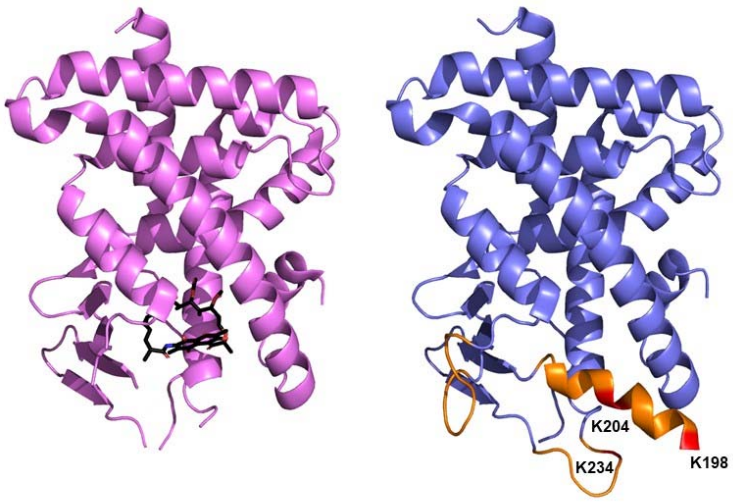

Figure S20. Flexibility of the ligand binding pocket of hPXR. The crystal structure of rifampicin-bound hPXR-LBD (PDB code 1SKX, pink) lacks density for several regions of the ligand binding pocket compared to the apo- structure of hPXR-LBD (PDB code 1ILG, blue). Amino acids 198-209, 229-235, and 310-317 (shown as orange in the apo structure) are not present in the rifampicin-bound structure model. Positions of K198, K204, and K234 are in red. Rifampicin is in black.

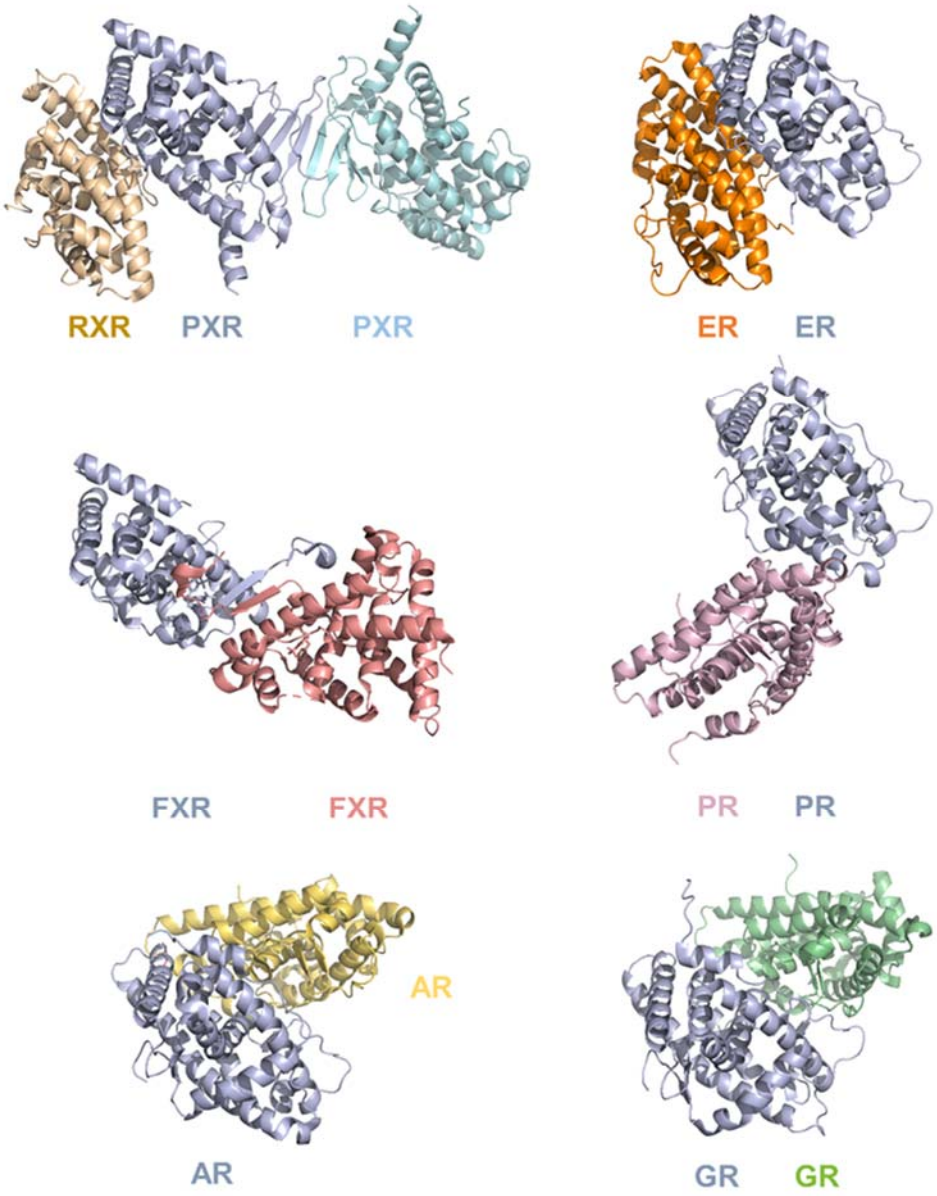

Figure S21. Homodimerization interfaces of nuclear receptors. The structure of the hPXR-RXR complex (PDB 4J5W) exemplifies the heterodimer interface shared by several nuclear receptors with their obligatory partner RXR. Certain nuclear receptors homodimerize using the same interface, such as estrogen receptor (ER, PDB 1QKU). Nuclear receptors that homodimerize using a different interface include farnesoid X receptor (FXR, PDB 4OIV), progesterone receptor (PR, PDB 1A28), androgen receptor (AR, 5JJM), and glucocorticoid receptor (GR, PDB 1M2Z). All homodimer structures were aligned to a hPXR monomer (light blue) in the RXR-hPXR-hPXR complex.

Upregulated genes in xenobiotic metabolism pathway		
Gene	**Log2FC**	**Adj. p value**
UGT2B15	9.52	1.60E-09
UGT2B10	8.05	3.10E-09
UGT2B4	7.83	1.25E-11
CYP3A7	7.72	8.91E-10
ADH1A	6.92	2.37E-07
UGT2B17	6.81	3.54E-08
ADH4	6.69	3.40E-09
CYP2C9	6.23	2.73E-11
CYP2C18	6.20	5.98E-11
UGT2B11	5.90	7.47E-07
UGT2B7	5.71	7.05E-10
CYP2E1	5.45	1.71E-06
UGT2A3	5.20	1.16E-12
CYP2B6	5.07	7.97E-07
CYP2C19	4.68	1.29E-09
CYP3A4	4.23	1.67E-12
AKR1C4	4.21	2.64E-08
CYP3A5	3.69	6.28E-09
CYP3A43	3.68	1.38E-06
ADH6	3.39	2.12E-09
ADH1B	3.33	1.21E-13
UGT1A8	2.73	8.54E-03
CYP2C8	2.72	2.38E-06
CYP1A1	2.53	1.04E-07
CYP2S1	1.85	2.28E-04
GSTA2	1.83	9.18E-12
UGT1A6	1.07	3.54E-10
GSTA1	1.05	6.22E-10

Table S1. Genes extracted from the enrichment pathway analysis of RNA-seq data in xenobiotic metabolism which are ≥ 2-fold upregulated (hPXR KO over WT). Log2FC, Log2(Fold Change); Adj. p value, adjusted p value.

Peptide	Interprotein crosslinked peptide (protein A – protein B)	Lysine position (protein) in the crosslinked peptide		MeroX Score	m/z	z	MS1 mass accuracy (ppm)
		Protein A	Protein B				
1	DQISLLKGAAF-KLQLQ	277 (PXR)	251 (CAR)	216	975.0270	2	2.7
2	FLYAKLLGLLAELR-DTTFSHFKNFR	311 (CAR)	170 (PXR)	180	794.9187	4	1.1
3	FLYAKLLGLLAELR-EEAAKWSQVR	311 (CAR)	198 (PXR)	165	745.9029	4	1
4	DSGGKEIFSLLPHMA-KLQLQ	234 (PXR)	251 (CAR)	160	796.7361	3	7
5	FLYAKLLGLLAELR-KLQLH	311 (CAR)	332 (PXR)	157	604.6050	4	0.7
6	FLYAKLLGLLAELR-KDLCSLK	311 (CAR)	204 (PXR)	135	660.8726	4	0.01
7	KLQLH-KLQLQ	332 (PXR)	251 (CAR)	128	712.9007	2	0.54

Table S2. Parameters obtained from crosslinking mass spectrometry. Seven interlinked peptides were validated as participating in intermolecular interactions between hPXR LBD and hCAR LBD. The MeroX score and MS1 mass accuracy reflect the reliability of the method. The mass-to-charge ratio (m/z) and the charge (z) corresponding to the interlinked peptides are indicated along the lysine residues involved in the reaction.

Peptide	Interprotein crosslinked peptide (protein A – protein B)	Lysine position (protein) in the crosslinked peptide		Distance (Å) between crosslinked lysine residues in the model	B factor values for the corresponding lysine residues	
		Protein A	Protein B		hPXR	hCAR
1	DQISLLKGAAF-KLQLQ	277 (PXR)	251 (CAR)	26	39	86
2	FLYAKLLGLLAELR-DTTFSHFKNFR	311 (CAR)	170 (PXR)	29	46	79
3	FLYAKLLGLLAELR-EEAAKWSQVR	311 (CAR)	198 (PXR)	44	82	79
4	DSGGKEIFSLLPHMA-KLQLQ	234 (PXR)	251 (CAR)	51	85	86
5	FLYAKLLGLLAELR-KLQLH	311 (CAR)	332 (PXR)	27	45	79
6	FLYAKLLGLLAELR-KDLCSLK	311 (CAR)	204 (PXR)	32	84	79
7	KLQLH-KLQLQ	332 (PXR)	251 (CAR)	38	45	86

Table S3. Crosslinking mass spectrometry studies determined distances spanned by the interlinked peptides. Distances between lysine pairs within crosslinked peptides were measured between α carbons in the hPXR LBD-hCAR LBD model. The b factor values were extracted from crystal structures of hPXR LBD (PDB code 1ILH) and hCAR LBD (PDB code 1XV9).